

# Radio Interferometric Studies of Cool Evolved Stellar Winds

A dissertation submitted to the University of Dublin  
for the degree of Doctor of Philosophy

**Eamon O’Gorman**

Supervisor: Dr. Graham M. Harper

Trinity College Dublin, September 2013

---

SCHOOL OF PHYSICS  
UNIVERSITY OF DUBLIN  
TRINITY COLLEGE



## Declaration

I declare that this thesis has not been submitted as an exercise for a degree at this or any other university and it is entirely my own work.

I agree to deposit this thesis in the University's open access institutional repository or allow the library to do so on my behalf, subject to Irish Copyright Legislation and Trinity College Library conditions of use and acknowledgement.

**Name:** Eamon O'Gorman

**Signature:** ..... **Date:** .....



## Summary

Mass-loss becomes significant for most stars as they approach the end of their lives and become either red giants or red supergiants. This continuous mass-loss, which occurs in the form of a relatively dense and slow-moving wind, can have a significant impact on the evolution of gas and dust in galaxies, on surrounding planets, and indeed on the very evolution of the star itself. Despite the importance of this phenomenon and decades of study, the fundamental mechanisms responsible for producing these winds remain unknown. The main reason for this is due to our lack of understanding of the dynamics and thermodynamics of the stellar outflow environment. Isolated giants and supergiants do not contain the expected additional complexities encountered by binaries, making them ideal targets for understanding the nature of these outflows. Traditionally, observations have provided only limited disk-averaged information about the outflow environments of these stars making it difficult to infer the outflow properties. However, the latest suite of radio interferometers now have the capability to provide essential spatial information on these outflow environments.

This thesis first presents the results of a radio interferometric study into the dynamics of the two unique flows in the circumstellar environment of the M2 red supergiant, Betelgeuse. The Combined Array for Research in Millimeter-wave Astronomy (CARMA) was used in multiple configurations to observe the CO( $J = 2 - 1$ ) emission line allowing spatial scales as small as  $0''.9$  to be traced over a  $32''$  field of view. The outer flow known as S2, was found to have outflow velocities of  $-15.4$  and  $+13.2$  km s $^{-1}$  with respect to the stellar rest frame and

extend out to  $17''$ , while the inner flow known as S1, was found to have outflow velocities of  $-15.4$  and  $+13.2 \text{ km s}^{-1}$  and extend out to  $4 \rightarrow 6''$ . Both flows were found to be inhomogeneous down to the resolution limit, but when azimuthally averaged, their intensity falloff was found to be consistent with an optically thin, spherically symmetric constant velocity outflow. High resolution multi-epoch centimeter continuum observations of Betelgeuse which probe its inner atmosphere ( $\sim 1 - 5 R_*$ ) are also presented. The radio flux density is found to vary on time scales of  $\lesssim 14$  months at all wavelengths, and again evidence for inhomogeneities in the outflow is found.

This thesis also presents Karl G. Jansky Very Large Array (VLA) multi-wavelength ( $0.7 - 20 \text{ cm}$ ) observations of two non-dusty, non-pulsating K spectral-type red giants, Arcturus and Aldebaran. Detections at  $10 \text{ cm}$  ( $3.0 \text{ GHz}$ : S-band) and  $20 \text{ cm}$  ( $1.5 \text{ GHz}$ : L-band) represent the first isolated luminosity class III red giants to be detected at these long wavelengths. These thermal continuum observations provide a snapshot of the different stellar atmospheric layers and are independent of any long-term variability. The long wavelength data sample Arcturus' outer atmosphere where its wind velocity is approaching its terminal value and the ionization balance is becoming *frozen-in*. For Aldebaran the data still sampling its inner atmosphere where the wind is still accelerating. Our data is in conflict with published semi-empirical models based on ultraviolet data. Spectral indices are used to discuss the possible properties of the stellar atmospheres. Evidence for a rapidly cooling wind in the case of Arcturus is found and a new analytical wind model is developed for this star. This model is used as the basis to compute a thermal energy balance of Arcturus' outflow by investigating the various heating and cooling processes that control its thermal structure. The analysis focuses on distances between  $1.2 \rightarrow 10 R_*$  and includes the wind acceleration zone. We find that an additional substantial heating mechanism is required to maintain the inner thermal structure of the outflow.

*For Mum and Dad,  
a constant source of inspiration and guidance.*

# Acknowledgements

Some sincere acknowledgements...

# List of Publications

## Refereed

1. **O’Gorman, E.**, Harper, G. M., Brown, A., Brown, A., Drake, S., and Richards, A. M. S.  
“Multi-wavelength Radio Continuum Emission Studies of Dust-free Red Giants”  
The Astronomical Journal, 146, 98, (2013)
2. Richards, A. M. S., Davis, R. J., Decin, L., Etoke, S., Harper, G. M., Lim, J. J., Garrington, S. T., Gray, M. D., McDonald, I., **O’Gorman, E.**, Wittkowski, M.  
“e-MERLIN resolves Betelgeuse at wavelength 5 cm”  
Monthly Notices of the Royal Astronomical Society Letters, 432, L61 (2013)
3. **O’Gorman, E.**, Harper, G. M., Brown, J. M., Brown, A., Redfield, S., Richter, M. J., and Requena-Torres, M. A.  
“CARMA CO(J = 2 - 1) Observations of the Circumstellar Envelope of Betelgeuse”  
The Astronomical Journal, 144, 36 (2012)
4. Sada, P. V., Deming, D., Jennings, D. E., Jackson, B. K., Hamilton, C. M., Fraine, J., Peterson, S. W., Haase, F., Bays, K., Lunsford, A., and **O’Gorman, E.**  
“Extrasolar Planet Transits Observed at Kitt Peak National Observatory”  
Publications of the Astronomical Society of the Pacific, 124, 212 (2012)



- 
5. Sada, P. V., Deming, D., Jackson, B. K., Jennings, D. E., Peterson, S. W., Haase, F., Bays, K., **O’Gorman, E.**, and Lundsford, A.  
“Recent Transits of the Super-Earth Exoplanet GJ 1214b”  
The Astrophysical Journal Letters, 720, L215 (2010)

## **Non-Refereed**

1. **O’Gorman, E.**, & Harper, G. M.  
“What is Heating Arcturus’ Wind?”,  
Proceedings of the 16th Cambridge Workshop on Cool Stars, Stellar Systems and the Sun. Astronomical Society of the Pacific Conference Series, 448, 691 (2011)

# Contents

<b>List of Publications</b>	<b>vii</b>
<b>List of Figures</b>	<b>x</b>
<b>List of Tables</b>	<b>xi</b>
<b>1 Conclusions and Future Work</b>	<b>1</b>
1.1 Principle Results . . . . .	2
1.1.1 Multi-wavelength Study of Betelgeuse’s Extended Atmosphere . . . . .	2
1.1.2 Multi-wavelength Radio Continuum Emission Studies of Dust-free Red Giants . . . . .	4
1.2 Future Work . . . . .	6
1.2.1 Probing the S1 flow of Betelgeuse with ALMA . . . . .	7
1.2.2 Multi-epoch centimeter observations of Betelgeuse . . . . .	9
1.2.3 Developing new atmospheric models for Arcturus and Aldebaran . . . . .	12
1.2.4 Karl G. Jansky VLA Survey of Red Giants . . . . .	12
<b>A List of Abbreviations Used in this Thesis.</b>	<b>14</b>
<b>B Discrete Absorption Feature</b>	<b>16</b>
<b>References</b>	<b>18</b>

## List of Figures

1.1	Simulating ALMA dust observations. . . . .	8
1.2	Simulating ALMA CO(J=6-5) observations. . . . .	8
1.3	MERLIN + “old” VLA image of Betelgeuse . . . . .	11
1.4	Block diagram for atmospheric model development. . . . .	13

# List of Tables

A.1 List of Abbreviations . . . . .	14
-------------------------------------	----

# 1

## Conclusions and Future Work

The goal of the thesis was to broaden our understanding of the outflow environments of red giants and red supergiants. To achieve this goal, we observed these stars with the most sensitive radio interferometers available, allowing their atmospheres to be probed with exquisite detail. The first part of the thesis described the results of our multi-wavelength high spatial resolution campaign to enhance our understanding of Betelgeuse’s complex outflow environment. The second part of the thesis focused on the analysis of multi-wavelength centimeter continuum emission from Arcturus and Aldebaran which provided a snapshot of the different stellar atmospheric layers. In this chapter, the primary findings and conclusions of these two studies are presented along with possible directions for future work.

## 1.1 Principle Results

The main findings of the thesis are discussed in the following two sections.

### 1.1.1 Multi-wavelength Study of Betelgeuse's Extended Atmosphere

- The two distinct velocity components seen by [Bernat \*et al.\* \(1979\)](#) in CO absorption against the stellar spectrum at  $4.6\ \mu\text{m}$  were both detected at 230 GHz for the first time. The extended CARMA C configuration resolved out almost all of the S2 emission leaving us with an approximate line profile for the S1 flow. From this profile a blueshifted outflow velocity of  $-9.0\ \text{km s}^{-1}$  and a slightly greater redshifted outflow velocity of  $+10.6\ \text{km s}^{-1}$  was inferred; in good agreement with [Bernat \*et al.\*'s \(1979\)](#) expansion velocity value of  $9\ \text{km s}^{-1}$ .
- The line profiles obtained with the D and E configurations were found to be wider than the C configuration line profile with the notable appearance of an extreme blue wing feature which was associated with the S2 flow. The high spectral resolution multi-configuration spectrum was used to determine S2 outflow velocities of  $-15.4\ \text{km s}^{-1}$  and  $+13.2\ \text{km s}^{-1}$  which are in good agreement with [Bernat \*et al.\*'s \(1979\)](#) value of  $16\ \text{km s}^{-1}$ .
- In the blueshifted channels of the multi-configuration image cube the emission is compact at high absolute velocities and becomes more extended at lower absolute velocities indicating that the S2 flow has a shell like structure. This is less clear in the redshifted channels indicating an asymmetrical shell. These multi-configuration maps provide the first direct measurements on the spatial extent of the S2 flow, which we derive to have a radius of  $17''$ ; a value that is higher than most previous estimates.
- A well defined outer edge for the S1 flow is not obvious. The emission at low absolute velocities is resolved out in the S1 line profile and because the resolving out scale of the C configuration is  $\sim 6''$ , this tells us that the spatial extent of the emission must be at least  $\sim 3''$ . From the intensity

distribution of the S1 emission, we infer that the extent of the S1 emission is between  $4 - 6''$ .

- Both flows were found to be inhomogeneous down to the resolution limit with a notable clump of emission  $\sim 5''$  S-W of the star, at low absolute velocities. However, when azimuthally averaged, the intensity falloff of both flows was found to be consistent with an optically thin, spherically symmetric constant velocity outflow.
- Previous single dish observations of the CO line with small HPBW do not show the classical resolved signature of high emission at large absolute velocities and low emission at low absolute velocities for two main reasons. Firstly, the S1 flow is still unresolved in these single dish observations and thus contributes emission and at the lower absolute velocities. As well as this, the multi-configuration CARMA maps show that the S2 emission is brighter in the higher absolute velocity maps than at lower absolute velocities and so when the emission from the fainter rings is neglected (i.e. when observed with a small HPBW), the overall line profile does not change significantly.
- The various CO rotational line profiles get narrower with increasing excitation energies indicating that the higher excitation lines are formed mainly in the S1 flow. Therefore the high frequency bands of ALMA will preferentially trace the S1 flow.
- Assuming a mean outflow velocity of  $14.3 \text{ km s}^{-1}$  and  $9.8 \text{ km s}^{-1}$  for the S2 and S1 flows, respectively, then their ages are  $\sim 1100 \text{ yr}$  and  $\sim 400 \rightarrow 600 \text{ yr}$ . The S1 flow may be an extension of the current wind phase seen at UV and centimeter wavelengths but higher spatial resolution data is needed to confirm this (see Section 1.2.1).
- The thermal continuum emission of Betelgeuse's inner atmosphere has been imaged at 6 cm with e-MERLIN, revealing two unresolved hotspots separated by 90 mas, with brightness temperatures  $5400 \pm 600$  and  $3800 \pm 500 \text{ K}$ .

The astrometric solutions of Harper *et al.* (2001) place the optical photospheric position almost directly at the position of the weaker feature meaning that the hotter feature is  $\sim 2 R_\star$  above the optical photosphere. Existing 1-D atmospheric models are capable of almost reproducing the low resolution e-MERLIN image but are inadequate at the highest e-MERLIN resolution. 1-D atmospheric models are probably not a realistic representation of Betelgeuse’s inner atmosphere.

- High spatial resolution multi-wavelength archival VLA+Pi Town data, taken 10 yr prior to the e-MERLIN data set, were examined to look for signatures of the e-MERLIN hotspots. No evidence was found for the presence of the two hotspots at either 1.3 or 0.7 cm where the resolution was comparable or better than that of e-MERLIN’s. We conclude that the hotspots are either optically thin at these high frequencies or their dynamics are time dependent on scales of just a few years.
- Multi-epoch, multi-wavelength radio continuum observations between 1996 and 2004 reveal total flux density variations between  $20 \rightarrow 35\%$  at wavelengths between 0.7 and 6 cm. The 0.7 cm radio maps show a highly asymmetric source at all epochs with dramatic changes in the radio emitting topology over a time period of only one to two years. These frequent changes in the radio emitting topology may be the cause of the flux density variations at 0.7 cm.

### 1.1.2 Multi-wavelength Radio Continuum Emission Studies of Dust-free Red Giants

- The thesis presented the most comprehensive set of multi-wavelength radio continuum observations of two luminosity class III red giants to date. A snapshot of the different stellar atmospheric layers of Arcturus and Aldebaran was obtained, independent of any long-term variability. The first detections were made at several wavelengths for each star including a detection at 10 cm (3.0 GHz: S-band) for both stars and a 20 cm (1.5 GHz: L-band) detection for Arcturus making these the first isolated luminosity class III red giants to be detected at such long wavelengths.



- The long-wavelength data sample the outer layers of Arcturus' atmosphere where its wind velocity is approaching its terminal value and the ionization balance is becoming frozen-in. For Aldebaran however, the long-wavelength data is still sampling its inner atmosphere where the wind is still accelerating probably due to its lower mass loss rate.
- Little evidence for radio flux variability was found when our measurements were compared with previous observations. However, previous observations have provided only a small number of modest S/N measurements and so it is difficult to make a conclusive statement regarding the radio variability of these sources. Interestingly, prior to this study Aldebaran had been observed at 6 cm but was not detected. However, we detected the star at 6 cm with a flux density over two times greater than the previous  $3\sigma$  upper limit, which could mean that its wind may have a time dependent nature.
- Our radio flux density measurements were compared with the predictions of published semi-empirical models based on UV data. The chromospheric and transition region semi-empirical model of [McMurry \(1999\)](#) with an optically thin wind overlain does well in reproducing our radio fluxes but we find that the chromospheric and wind semi-empirical model of [Drake \(1985\)](#) does not agree well with our data.
- Arcturus was found to have a spectral index of  $\alpha = 1.05 \pm 0.05$  while Aldebaran's value was found to be higher at  $\alpha = 1.58 \pm 0.25$ . Both of these values are well above that expected for an isothermal wind with a constant velocity and ionization fraction.
- The long wavelength radio measurements of Arcturus were found to be emanating from a region of the atmosphere where its wind is close to the terminal velocity. This allowed evidence to be found for a rapidly cooling wind with a temperature,  $T(r) \propto r^{1.65}$ .
- A new wind model was developed for Arcturus which was based on the analytical advection model of [Glassgold & Huggins \(1986\)](#). It incorporating

a rapidly cooling wind profile and was based on the new VLA long wavelength flux measurements. This provided a new *hybrid* atmospheric model for Arcturus which consists of the original inner atmosphere developed by Drake (1985) out to a radius of  $2.3 R_{\star}$  and the new wind model further out.

- The new hybrid atmospheric model for Arcturus was used to investigate the various heating and cooling processes that control the thermal structure of its mass outflow region between  $1.2 \rightarrow 10 R_{\star}$ . Lyman  $\alpha$  line cooling was found to be the main cooling mechanism within  $2.8 R_{\star}$  while adiabatic expansion cooling was the most efficient cooling mechanism further out. Magnetic wave heating, caused by the cascade of energy from large to small eddies, is found to be the main heating mechanism throughout the atmosphere. A
- A considerable net cooling was calculated at all distances from the star. Within  $\sim 3 R_{\star}$ , this net cooling far exceeds that predicted by the atmospheric model implying that one or more additional energy inputs must be acting on the inner region of the outflow to maintain the thermal profile. Beyond  $\sim 3 R_{\star}$ , the only significant cooling process is adiabatic expansion which is insufficient to account for the super-adiabatically cooling wind.

## 1.2 Future Work

Many past studies of cool evolved stars have been carried out in the UV with space based observatories. With no dedicated space based missions in the UV planned for the near future, studies of these stars at other wavelengths will become increasingly common and important. The thesis has shown that important and exciting science can be carried out with these stars at radio wavelengths using the latest suite of radio interferometers. The main findings of the thesis have been based on observations carried out with the most sensitive millimeter and centimeter interferometers available at the time. The CARMA millimeter interferometer is currently being surpassed in sensitivity, spatial and spectral resolution, and frequency coverage by the Atacama Large Millimeter/submillimeter Array (ALMA). ALMA will open up a whole new part of the millimeter and

submillimeter spectrum for study with exquisite detail, allowing the distribution of molecules and dust around these stars to be mapped with resolution of just a few milliarcseconds at the highest frequencies. Most of the centimeter observations discussed in previous chapters were obtained with the VLA and e-MERLIN during their commissioning phase with only a fraction of the now available bandwidth. The large bandwidth now available with these instruments will allow fast detections of historically weak or undetectable radio continuum luminosity class III red giants at both long and short wavelengths. Previous upper limits will be replaced by firm detections allowing a greater understanding of their outer atmospheric properties. In the following sections we describe some future projects which would complement and improve on the work carried out within this thesis.

### 1.2.1 Probing the S1 flow of Betelgeuse with ALMA

Chapter ?? outlined how the inner S1 flow around Betelgeuse was successfully imaged with sub-arcsecond spatial resolution (i.e.,  $0.9''$ ), revealing an irregular CO distribution between  $40 R_\star$  ( $0.9''$ ) and  $270 R_\star$  ( $\sim 6''$ ). Recently, [Kervella et al. \(2011\)](#) recorded a series of thermal IR images using the VLT/VISIR ( $\lambda = 8 - 20 \mu\text{m}$ ) and found a ring-like structure at radius  $0.5 - 1.0''$  (i.e.,  $\sim 30 R_\star$ ) which the author associated with the dust condensation radius. Such a spatial scale was just beyond the resolution of our CARMA data set. To build a complete and consistent picture of the mass-loss in Betelgeuse we have been awarded 5.5 hours of observing time with ALMA in the current observing cycle (i.e., ALMA Early Science Cycle 1). The goal of this future study is to unravel the dynamical and chemical structure of the inner CSE ( $\lesssim 3''$ ) via observations of molecular line emission with a resolution of  $\sim 0.09''$ , an order of magnitude greater than our CARMA study. Such observations will shed light on the spatial correlation between the dust and molecules in the CSE and may identify the region where molecules condense into dust grains.

The observations will be carried out in the extended configuration ( $B_{\text{max}} \sim 1 \text{ km}$ ) and the main target line will be the CO( $J = 6 - 5$ ) line at 691 GHz. CO is a very stable molecule and does not take part in dust condensation allowing us to distinguish between different chemical and dynamics effects. Figure 1.1 displays a

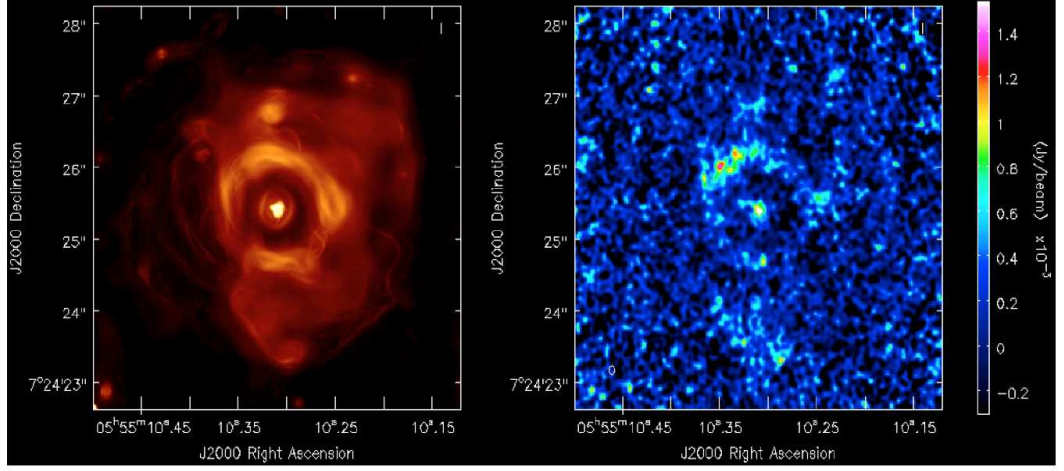


**Figure 1.1:** *Left:* Dust emission model based on the the VLT/VISIR image of [Kervella \*et al.\* \(2011\)](#) showing a ring like structure which may be the region of dust condensation around Betelgeuse. *Right:* Simulated ALMA image of 6 GHz of continuum emission after two hours on source reveals that some of the structure should be detectable.

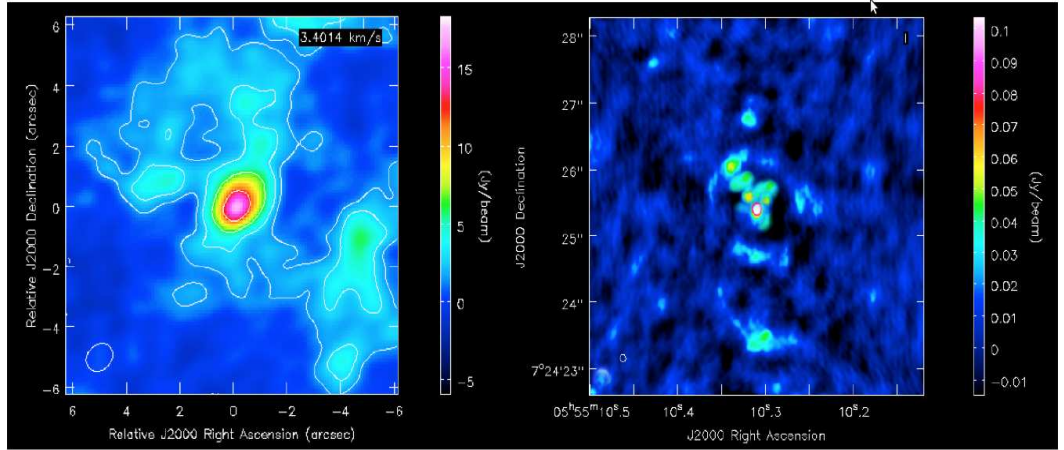


**Figure 1.2:** *Right:* Channel map from the CO( $J = 2-1$ ) image cube of [O’Gorman \*et al.\* \(2012\)](#) using CARMA with a resolution of  $0.9''$ . *Right:* CASA simulator tool image of the CARMA channel map scaled according to the Herschel CO( $J = 6-5$ ) emission line flux (see Chapter ??) while assuming to have structure on the same scales as the dust.

dust emission model based on the the VLT/VISIR image of [Kervella \*et al.\* \(2011\)](#) showing a ring like structure which may be the region of dust condensation around Betelgeuse. This image was inputted into the CASA simulation tool to create an image of the expected ALMA dust observations, assuming 6 GHz of line-free continuum close to 690 GHz. In just 2 hours of observing time we expect to be able to detect this structure. Figure 1.2 (left) shows a channel map from our final CARMA CO( $J = 2 - 1$ ) image cube. We scaled the intensity of this map according to the Herschel CO( $J = 6 - 5$ ) line flux and assumed that the CO has the same structure on the same scales as the dust. Figure 1.2 (right) shows the simulated distribution and brightness of the CO( $J = 6 - 5$ ) which indicates that we will be able to locate individual clump emission with a  $0.09''$  beam. Even though the S1 flow is expected to extend out to  $\sim 6''$ , the CO( $J = 6 - 5$ ) will be more concentrated than the CO( $J = 2 - 1$ ) emission and most of the strongest CO( $J = 6 - 5$ ) emission will be within the  $9''$  ALMA primary beam.

### 1.2.2 Multi-epoch centimeter observations of Betelgeuse

The recent e-MERLIN 5.2 cm continuum image of Betelgeuse by [Richards \*et al.\* \(2013\)](#) has made the surprise discovery that the inner atmosphere contains two hotspots separated by 90 mas (i.e.,  $4 R_\star$ ). A number of outstanding issues remain in explaining the origin of these features. The first issue is that the exact position of the optical photosphere is uncertain. While [Richards \*et al.\* \(2013\)](#) assumed this position to be at the source peak of a lower resolution image, we have shown that the astrometric solution of [Harper \*et al.\* \(2008\)](#) places the optical photosphere almost directly at the position of the less bright hotspot, which would mean that the brightest feature is located  $\sim 3 R_\star$  above the optical photosphere. However, this astrometric solution was based in part on lower resolution radio data and so does not contain the desired level of precision. Another issue is that the time scales over which these features vary, in both brightness and position, are completely unknown. Along with the uncertainty in the photospheric position, the problem is that the velocity profile of the inner atmosphere is uncertain, due to traditional UV line diagnostics being contaminated by the large turbulent velocity while also being disk averaged measurements.

Our VLA–Pie Town data have revealed significant flux variations at all observed wavelengths on time scales as short as 14 months (the observing interval), while Drake *et al.* (1992) found similar variations on time scales as short as 40 days. The source of these variations will be strongly associated with these hot spots, at C-band at least, as Richards *et al.* (2013) has shown that these contain most of the total radio flux. Ohnaka *et al.* (2011) created a 1-D aperture synthesis image of Betelgeuse using the VLTI/AMBER and concluded that “the outer atmosphere extending to  $\sim 1.3 - 1.4 R_\star$  is asymmetric and its dynamics is dominated by vigorous, inhomogeneous large-scale motions, whose overall nature changes drastically within one year”. Could it be possible that the hotspots seen at radio wavelengths also change drastically within one year? Either way they are likely linked to the wind-driving mechanism.

**Table 1.1:** Relevant capabilities of the VLA and e-MERLIN for future multi-epoch observations of Betelgeuse

	e-MERLIN (C band)	e-MERLIN (K band)	VLA (C band)	VLA (K band)
Resolution <sup>1</sup> (mas)	40	12	330	90
Frequency range (GHz)	4 – 8	22 – 24	4 – 8	18 – 26.6
Bandwidth (GHz)	2	2	4	8
Sensitivity <sup>2</sup> ( $\mu$ Jy/bm)	$\sim 2$	$\sim 15$	$\sim 2$	$\sim 2$
Maximum Scale (")	$\sim 0.75$	$\sim 0.16$	$\sim 8.9$	$\sim 2.4$

<sup>1</sup> Using uniform weighting. <sup>2</sup> Eight hour observing run.

Spatial resolution is a key requirement to understand the dynamics and evolution of these hotspots and e-MERLIN is the most suited instrument for future radio studies. e-MERLIN is expected to operate at K-band by 2014 and so a future study consisting of both C and K band observations would be preferable as each frequency would probe different layers of the atmosphere, potentially detecting other unique hotspots. Table 1.1 summarizes the relevant capabilities of e-MERLIN for such a study. The additional K band observations would have a maximum resolution of 12 mas providing 10 resolution elements across the radio

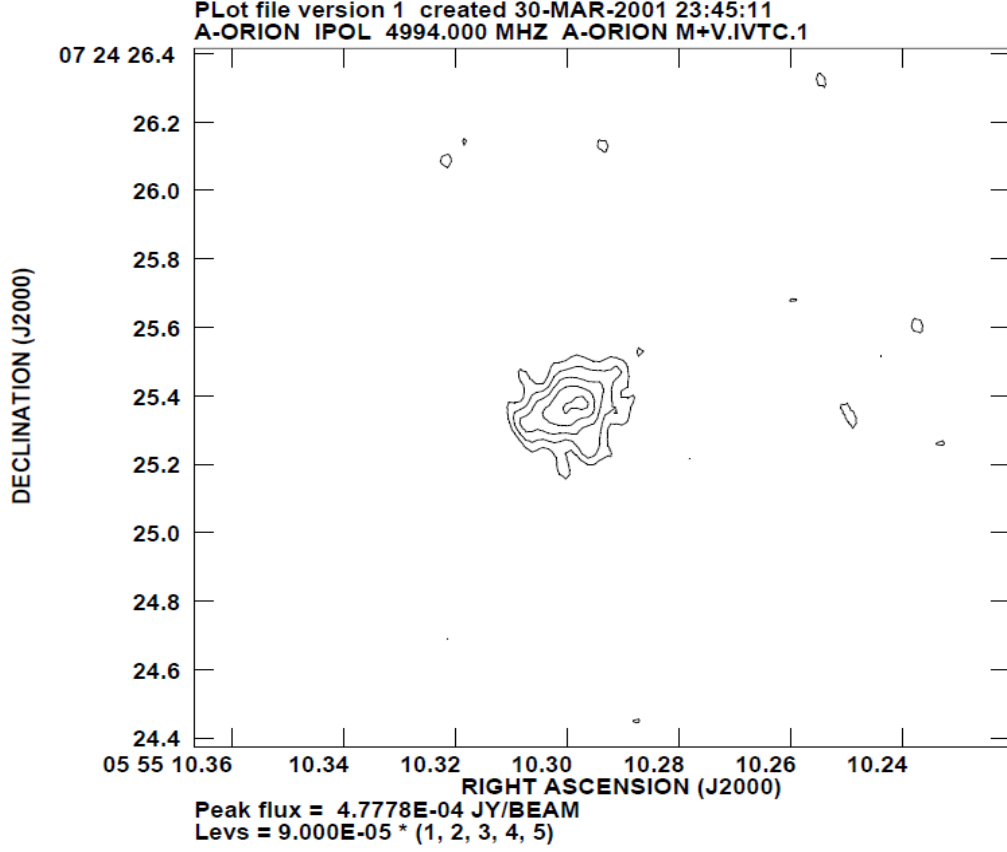


**Figure 1.3:** Combined MERLIN and “old” VLA image of Betelgeuse at C band. The MERLIN data was taken between 3 – 5th and 13 – 14 November 1996, while the VLA data was obtained on the 21st October, one and two weeks prior to the MERLIN data. The maximum resolution is 57 mas and the rms noise level is unknown. Contour levels are at  $(1, 2, 3, 4, 5) \times 90$  mJy. Extended emission exits on scales of  $\sim 400$  mas while the inner emission is asymmetric in the same direction as the new e-MERLIN data, although the distribution of the intensity appears to be different. The recent upgrades to the VLA now provides  $\sim 40$  times more bandwidth than used to create this image. Figure courtesy of Dr. Rhys Morris.

disk<sup>1</sup>. Multi-epoch observations will be required to study the evolution of these features. Based on the conclusions of Ohnaka *et al.* (2011) along with the substantial flux variations we see in the radio, it would seem appropriate to carry out 3 – 4 unique observations at both C and K band in one year. Richards *et al.*

<sup>1</sup>Based on the K band diameter of our VLA+Pie Town data.



(2013) C band observations were approximately 10 hr in total duration and used a total bandwidth of 0.5 GHz. Assuming the availability of the full 2 GHz of bandwidth at both C and K band then, in order to reach similar levels of sensitivity, three unique epochs each consisting of C and K band observations would amount to 30 hours of requested time with e-MERLIN.

Figure 1.4 shows a combined MERLIN and “old” VLA image of Betelgeuse at C band from 1996. Extended emission exists on scales of  $\sim 400$  mas while the inner emission is asymmetric in the same direction as the new e-MERLIN data, although the distribution of the intensity appears to be different. Extended emission was also detected in the e-MERLIN map in the form of a S-W arc as described in Chapter ???. The shorter baselines of the VLA would be more sensitive to this extended emission than e-MERLIN and so, combining VLA data with e-MERLIN data would surely produce the most detailed radio map of Betelgeuse ever produced. Obtained observing time with the VLA at both C and K band which coincide with the proposed e-MERLIN observations would be a challenge, especially considering that both instruments are dynamically scheduled. A more realistic option would be to apply for one epoch of VLA time to coincide with one of the e-MERLIN observing blocks. The extended emission will evolve on slower timescales anyway, and so one epoch would be sufficient to create a detailed map of the extended emission.

### 1.2.3 Developing new atmospheric models for Arcturus and Aldebaran

e-merlin could constrain temp

### 1.2.4 Karl G. Jansky VLA Survey of Red Giants



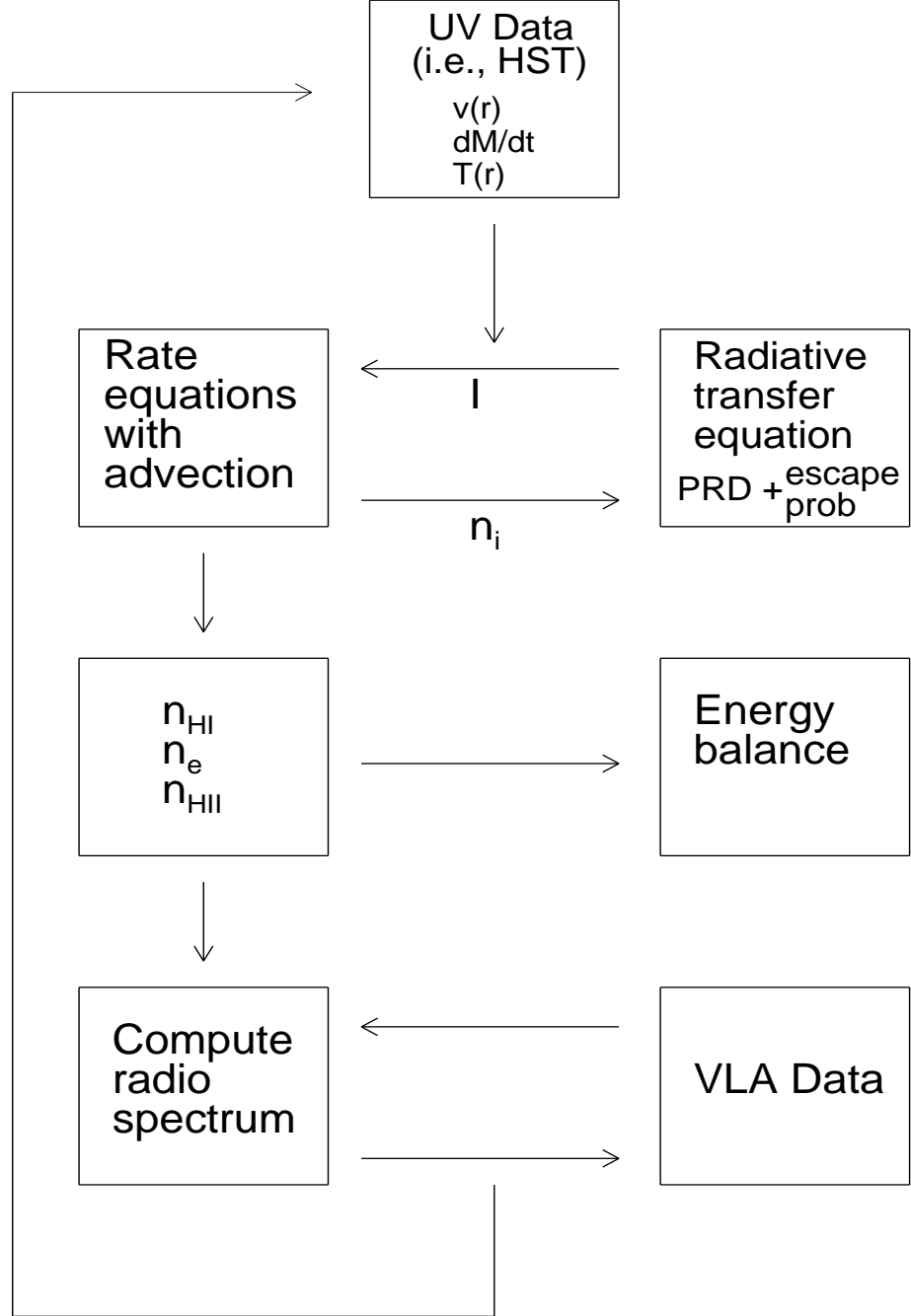


**Figure 1.4:** Block diagram summarizing the various stages involved in calculating a new atmospheric model for Arcturus and Aldebaran. The input model (starting guess) is mainly based on UV diagnostics. The radiative transfer equation and non-LTE atomic level populations (which include advection) are then simultaneously solved, and a radio spectrum is computed from the densities which is compared to the VLA data. The input model is gradually varied until the computed radio spectrum agrees with our VLA observations.



## List of Abbreviations Used in this Thesis.

**Table A.1:** List of Abbreviations

<b>Acronym</b>	<b>Meaning</b>
ALMA	The Atacama Large Millimeter/submillimeter Array
AGB	Asymptotic Giant Branch
BIMA	Berkeley Illinois Maryland Association
CARMA	Combined Array for Research in Millimeter-wave Astronomy
CSE	Circumstellar Envelope
DDT	Director's Discretionary Time
e-MERLIN	e-Multi-Element Radio Linked Interferometer Network
FOV	Field of View
GHRS	Goddard High-Resolution Spectrograph
GREAT	German Receiver for Astronomy at Terahertz Frequencies
HPBW	Half Power Beamwidth
H-R	Hertzprung-Russell
HST	Hubble Space Telescope
IOTA	Infrared Optical Telescope Array
IR	Infrared
IRAM	Institut de Radioastronomie Millimétrique
IUE	International Ultraviolet Explorer
LSR	Local Standard of Rest

*Continued on next page*

---

Table A.1 – *Continued from previous page*

<b>Acronym</b>	<b>Meaning</b>
LTE	Local Thermodynamic Equilibrium
MEM	Maximum Entropy Method
MHD	Magnetohydrodynamic
OVRO	Owens Valley Radio Observatory
OSRO	Open Shared Risk Observing
RF	Radio Frequency
RFI	Radio Frequency Interference
RGC	Red Giant Clump
RGB	Red Giant Branch
RSG	Red Supergiant
S/N	signal-to-noise ratio
SGB	Subgiant Branch
SOFIA	Stratospheric Observatory for Infrared Astronomy
SMA	Submillimeter Array
SZA	Sunyaev-Zel'dovich Array
SIS	superconductorinsulatorsuperconductor
UV	Ultraviolet
VLA	Karl G. Jansky Very Large Array
VLBA	Very Long Baseline Array
VLT	Very Large Telescope
W-R	Wolf-Rayet

---

# B

## Discrete Absorption Feature

The temperature equation outlined in Chapter ?? assumes that the wind is homogenous, but this may not be the case for Arcturus. During this study we analyzed STIS spectra of Arcturus from the online StarCAT catalog (Ayes, 2010). The Mg II *h* and *k* lines from data obtained in 2001 show a wind velocity  $\sim 30 - 40 \text{ km s}^{-1}$ , which is similar to that adopted in the Drake models for this star Drake (1985). A narrow discrete absorption feature is found at  $-49 \text{ km s}^{-1}$  in the broad blue-shifted wind absorption component of both lines as shown in Figure B.1. For this discrete feature we find a most probable turbulent velocity of  $3.4 \text{ km s}^{-1}$  and a Mg column density<sup>1</sup> of  $1.4 \times 10^{12} \text{ cm}^{-2}$ . A Mg column density of  $10^{15} \text{ cm}^{-2}$  is required to produce the blueward absorption components in the *h* and *k* lines (McClintock *et al.*, 1978). Therefore, this discrete absorption feature accounts for  $\sim 0.1\%$  of the total wind column density.

---

<sup>1</sup>Assuming all Mg to be Mg II

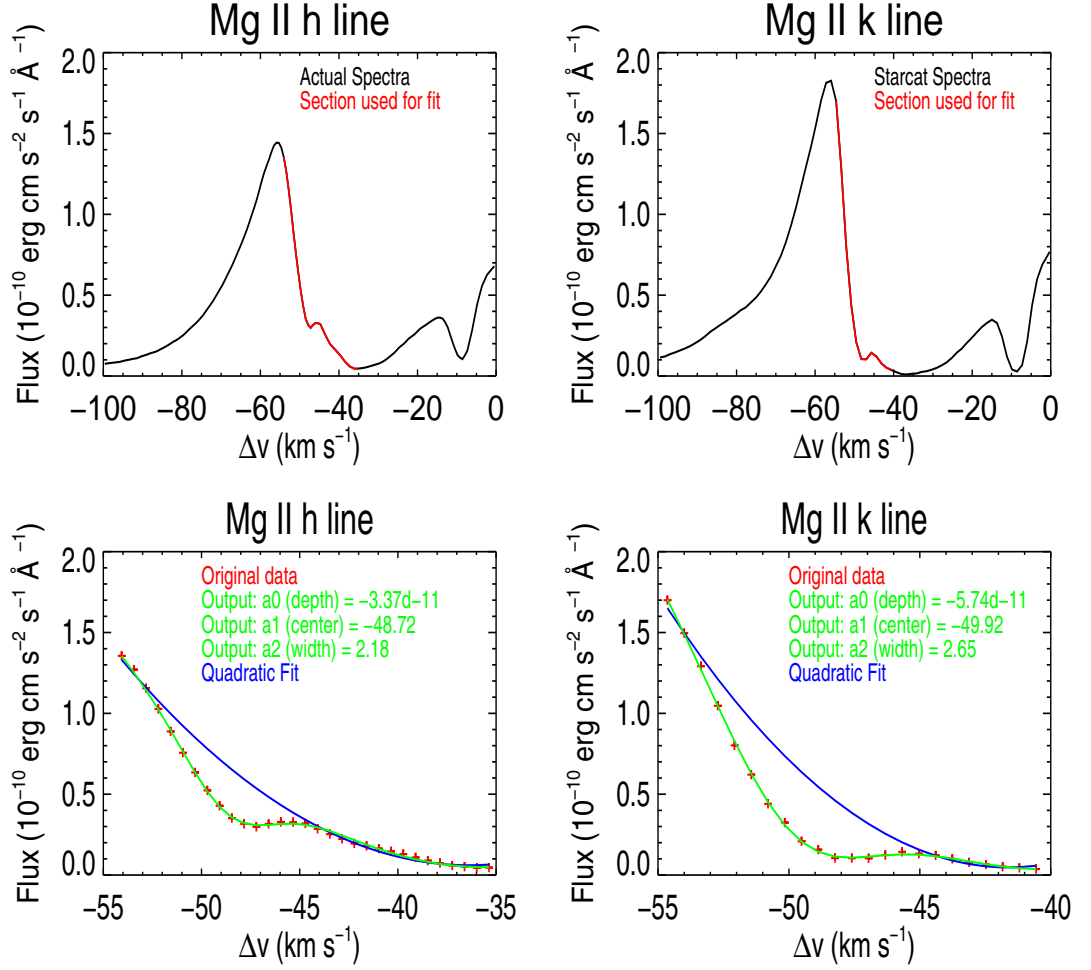


**Figure B.1:** Analysis on the absorption feature found in the Mg II *h* and *k* lines. A function composed of a linear combination of a Gaussian and a quadratic fitted the discrete absorption feature the best. The red data in the upper row shows the data that is used in this analysis.

# References

- AYRES, T.R. (2010). StarCAT: A Catalog of Space Telescope Imaging Spectrograph Ultraviolet Echelle Spectra of Stars. *Astrophysical Journal Supplemental Series*, **187**, 149–171. (Cited on page 16.)
- BERNAT, A.P., HALL, D.N.B., HINKLE, K.H. & RIDGWAY, S.T. (1979). Observations of CO circumstellar absorption in the 4.6 micron spectrum of Alpha Orionis. *Astrophysical Journal Letters*, **233**, L135–L139. (Cited on page 2.)
- DRAKE, S.A. (1985). Modeling lines formed in the expanding chromospheres of red giants. In J.E. Beckman & L. Crivellari, eds., *Progress in stellar spectral line formation theory; Proceedings of the Advanced Research Workshop, Trieste, Italy, September 4-7, 1984 (A86-37976 17-90)*. Dordrecht, D. Reidel Publishing Co., 1985, p. 351-357. (Cited on pages 5, 6 and 16.)
- DRAKE, S.A., BOOKBINDER, J.A., FLORKOWSKI, D.R., LINSKY, J.L., SIMON, T. & STENCEL, R.E. (1992). Four Years of Monitoring a Orionis with the VLA: Where have all the Flares Gone? In M. S. Giampapa & J. A. Bookbinder, ed., *Cool Stars, Stellar Systems, and the Sun*, vol. 26 of *Astronomical Society of the Pacific Conference Series*, 455. (Cited on page 10.)
- GLASSGOLD, A.E. & HUGGINS, P.J. (1986). The ionization structure of the circumstellar envelope of Alpha Orionis. *Astrophysical Journal*, **306**, 605–617. (Cited on page 5.)
- HARPER, G.M., BROWN, A. & LIM, J. (2001). A Spatially Resolved, Semiempirical Model for the Extended Atmosphere of  $\alpha$  Orionis (M2 Iab). *Astrophysical Journal*, **551**, 1073–1098. (Cited on page 4.)
- HARPER, G.M., BROWN, A. & GUINAN, E.F. (2008). A New VLA-Hipparcos Distance to Betelgeuse and its Implications. *Astronomical Journal*, **135**, 1430–1440. (Cited on page 9.)
- KERVELLA, P., PERRIN, G., CHIAVASSA, A., RIDGWAY, S.T., CAMI, J., HAUBOIS, X. & VERHOELST, T. (2011). The close circumstellar environment of Betelgeuse. II. Diffraction-limited spectro-imaging from 7.76 to 19.50  $\mu\text{m}$  with VLT/VISIR. *Astronomy & Astrophysics*, **531**, A117. (Cited on pages 7, 8 and 9.)
- MCCINTOCK, W., MOOS, H.W., HENRY, R.C., LINSKY, J.L. & BARKER, E.S. (1978). Ultraviolet observations of cool stars. VI - L alpha and MG II emission line profiles (and a search for flux variability) in Arcturus. *Astrophysical Journal Supplemental Series*, **37**, 223–233. (Cited on page 16.)

## REFERENCES

---

- McMURRY, A.D. (1999). The outer atmosphere of Tau - I. A new chromospheric model. *Monthly Notices of the Royal Astronomical Society*, **302**, 37–47. (Cited on page [5](#).)
- O’GORMAN, E., HARPER, G.M., BROWN, J.M., BROWN, A., REDFIELD, S., RICHTER, M.J. & REQUENA-TORRES, M.A. (2012). CARMA CO(J = 2 - 1) Observations of the Circumstellar Envelope of Betelgeuse. *Astronomical Journal*, **144**, 36. (Cited on page [8](#).)
- OHNAKA, K., WEIGELT, G., MILLOUR, F., HOFMANN, K.H., DRIEBE, T., SCHERTL, D., CHELLI, A., MASSI, F., PETROV, R. & STEE, P. (2011). Imaging the dynamical atmosphere of the red supergiant Betelgeuse in the CO first overtone lines with VLTI/AMBER. *Astronomy & Astrophysics*, **529**, A163. (Cited on pages [10](#) and [11](#).)
- RICHARDS, A.M.S., DAVIS, R.J., DECIN, L., ETOKA, S., HARPER, G.M., LIM, J.J., GARRINGTON, S.T., GRAY, M.D., McDONALD, I., O’GORMAN, E. & WITKOWSKI, M. (2013). e-MERLIN resolves Betelgeuse at  $\lambda$  5 cm: hotspots at 5 R. *Monthly Notices of the Royal Astronomical Society*, **432**, L61. (Cited on pages [9](#), [10](#) and [11](#).)